Increased DNA Damage and Apoptosis in CDKL5-Deficient Neurons

INCREASED DNA DAMAGE AND APOPTOSIS IN CDKL5-DEFICIENT NEURONS

Manuela Loi*, Stefania Trazzi*, Claudia Fuchs, Giuseppe Galvani, Giorgio Medici, Laura Gennaccaro, Marianna Tassinari, Elisabetta Ciani.

Department of Biomedical and Neuromotor Sciences, University of Bologna, Italy.

* Authors labeled with an asterisk contributed equally to the work.

Corresponding authors:

Elisabetta Ciani, Department of Biomedical and Neuromotor Sciences, Piazza di Porta San Donato 2, 40126 Bologna, Italy. Tel +39 0512091773; Fax +39 0512091737; e-mail: elisabetta.ciani@unibo.it

Stefania Trazzi, Department of Biomedical and Neuromotor Sciences, Piazza di Porta San Donato 2, 40126 Bologna, Italy. Tel +39 0512091773; Fax +39 0512091737; e-mail: stefania.trazzi3@unibo.it

Short/running title: CDKL5 loss results in DNA damage signals

Keywords: CDKL5, neuronal maturation, oxidative stress, DNA damage, γH2AX.

ABSTRACT

Mutations in the *CDKL5* gene, that encodes a serine/threonine kinase, causes a rare encephalopathy, characterized by early-onset epilepsy and severe intellectual disability, named CDKL5 deficiency disorder (CDD). *In vitro* and *in vivo* studies in mouse models of Cdkl5 deficiency have highlighted the role of CDKL5 in brain development and, in particular, in the morphogenesis and synaptic connectivity of hippocampal and cortical neurons. Interestingly, CDKL5 deficiency in mice increases vulnerability to excitotoxic stress in hippocampal neurons. However, the mechanism by which CDKL5 controls neuronal survival is far from being understood. To investigate further the function of CDKL5 and dissect the molecular mechanisms underlying neuronal survival, we generated a human neuronal model of CDKL5 deficiency, using CRISPR/Cas9-mediated genome editing. We demonstrated that *CDKL5* deletion in human neuroblastoma SH-SY5Y cells not only impairs neuronal maturation, but also reduces cell proliferation and survival, with alterations in the AKT and ERK signaling pathways and an increase in the pro-apoptotic BAX protein and in DNA damage-associated biomarkers (i.e. γH2AX, RAD50 and PARP1). Furthermore, CDKL5-deficient cells were hypersensitive to DNA damage-associated stress, accumulated more DNA damage foci (γH2AX positive) and were more prone to cell death than the controls. Importantly, increased KA-induced cell death of hippocampal neurons of *Cdkl5* KO mice correlated with an increased γH2AX immunostaining. The results suggest a previously unknown role for CDKL5 in DNA damage response that could underlie the pro-survival function of CDKL5.

INTRODUCTION

CDKL5 deficiency disorder (CDD; OMIM 300203, 300672) is a severe developmental encephalopathy caused by mutations in the cyclin-dependent kinase-like 5 (*CDKL5*) gene [1,2]. This gene is located on the short arm of the X-chromosome [3] and encodes a serine/threonine kinase that is highly expressed in the brain [4,5]. All the clinical symptoms commonly associated with *CDKL5* mutations are related to a dysfunction of the central nervous system and include early-onset refractory epilepsy, hypotonia, severe intellectual disability, autistic features, and visual impairment [6,1,7,8].

To date, several pathogenic *CDKL5* mutations have been described, including deletions, truncations, splice variants, and missense variants [9,10]. It is commonly assumed that most of these mutations lead to a lack of CDKL5 protein expression. Thereby, to mimic the common defects in this disease, *Cdkl5* knockout (KO) mouse models were generated in order to elucidate the functions of CDKL5 [11-14]. Studies in *Cdkl5* KO mice have shown reduced neuronal branching accompanied by reduced spine density and maturation in the hippocampus, visual cortex, somatosensory, and perirhinal cortex [11,15-19], suggesting a role of CDKL5 in dendritic morphogenesis and synapse development. The synaptic localization of CDKL5 [20,21] and its binding to PSD-95 [20], strongly suggest that CDKL5 participates in excitatory synapse development and function. Indeed, functional consequences of CDKL5 deficiency in synaptic function and plasticity, and impaired long-term potentiation, have recently been reported in different *Cdkl5* deficient mouse models [17,18,13], suggesting the importance of synapse dysfunction as a determinant of CDD. The mechanisms underlying the role of CDKL5 in maintaining synaptic structure and function are starting to be delineated, and include signaling involved in the regulation of synaptic morphogenesis, such as BDNF-Rac1, BDNF-PLCγ1, AKT/mTOR and AKT/GSK3β [18,22].

In view of the variety of cellular processes regulated by protein kinases and of the severity of the neurological phenotype of CDD patients, it is widely assumed that CDKL5 may have a very complex role in neurons. Therefore, the function of CDKL5 in the brain is still far from being fully understood. Recent evidence reported a new role of CDKL5 in neuronal survival [23]. It was demonstrated that CDKL5 deficiency increases the vulnerability of neural cells to different neurotoxic/excitotoxic stimuli [23]. However, the mechanism by which CDKL5 controls neuronal survival is not fully understood.

Using a newly-generated human cellular model of CDKL5 deficiency, CRISPR-induced CDKL5 KO SH-SY5Y cells, we analyzed the cellular and molecular consequences of *CDKL5* gene loss. Our findings emphasize the importance of CDKL5 in neuronal maturation and survival, and highlight a previously unknown role for CDKL5 in DNA damage repair.

MATERIALS AND METHODS

Cell line and treatments

Human neuroblastoma cell line SH-SY5Y, deriving from The European Collection of Authenticated Cell Cultures (ECACC), was obtained from Sigma-Aldrich, and was maintained in Dulbecco Modified Eagle Medium (DMEM) supplemented with 10% heat-inactivated FBS, 2 mM of glutamine, and antibiotics (penicillin, 100 U/ml; streptomycin, 100 µg/ml), in a humidified atmosphere of 5% of CO_2 at 37°C. Cell medium was replaced every 3 days and the cells were sub-cultured once they reached 90% confluence.

Transfection and selection of CDKL5 knockout (KO) clones – SH-SY5Y cells were co-transfected with the hCDKL5 CRISPR/Cas9 KO plasmid and the hCDKL5 HDR plasmid (Santa Cruz Biotechnology),

using Lipofectamine 2000 reagent (Thermo Fisher Scientific). hCDKL5 CRISPR/Cas9 KO plasmid consists of a pool of 3 plasmids, each encoding the Cas9 nuclease and a target-specific 20 nt guide RNA (gRNA) designed to cause a double-strand break in the 5' constitutive exons (exon 1 and exon 2) within the hCDKL5 gene. The hCDKL5 HDR plasmid allows for the incorporation of a puromycin resistance gene in the site-specific Cas9-induced DNA cleavage within the human CDKL5 gene. Independent clones (SH-CDKL5-KOs) were selected and maintained in 1 μg/ml puromycin (Sigma-Aldrich).

Adenovirus infection - Cells were infected with CDKL5-FLAG adenovirus particles (ad-CDKL5; Vector BioLabs) or GFP adenovirus particles as a control (ad-GFP; Vector BioLabs) at 100 multiplicities of infection (MOI).

Hydrogen peroxide treatment - Cells were plated onto poly-D-lysine coated slides in a 6-well plate at density of 2.5×10^5 cells per well in culture medium supplemented with 10% FBS. The day after, cells were exposed to an increasing concentration of H_2O_2 (Sigma-Aldrich) for 24 h.

Serum withdrawal - Cells were plated onto poly-D-lysine coated slides in a 6-well plate at density of 2×10^5 cells per well in culture medium supplemented with 10% FBS. The day after cultures were rinsed with PBS and incubated for 24 or 48 h in serum free DMEM medium.

Retinoic acid and BDNF-induced differentiation - For differentiation analyses cells were plated onto poly-D-lysine coated slides in a 6-well plate at density of 1×10^5 cells per well in culture medium supplemented with 10% FBS. Twenty-four h after cell plating, cell differentiation was induced by adding 10 μM retinoic acid (RA; Sigma-Aldrich) each day for 5 days. After 5 days of RA-induced differentiation the cell medium was replaced with serum-free medium containing 50ng/ml of human recombinant BDNF (Biovision Inc.). BDNF was added daily to the culture medium for 7 days. Cells were fixed in a 4% paraformaldehyde 4% glucose solution at 37°C for 30 min.

Colony

Mice were handled according to protocols approved by the Italian Ministry for Health (approval number DGSAF 477/2019). The mice used in this work derive from the *Cdkl5* KO strain in the C57BL/6N background developed in [11] and backcrossed in C57BL/6J for three generations. Mice for testing were produced as previously described [24]. The day of birth was designated as postnatal day (P) zero and animals with 24 h of age were considered as 1-day-old animals (P1). Mice were housed 3-5 per cage on a 12 h light/dark cycle in a temperature-controlled environment with food and water provided *ad libitum.*

Primary hippocampal cultures and treatments

Primary hippocampal neuronal cultures were prepared from P1 *Cdkl5* +/Y and *Cdkl5* -/Y mice as previously described [24]. Approximately 1.2 x 10^5 cells were plated on coverslips coated with poly-L-lysine in 6-well plates and cultured in Neurobasal medium supplemented with B27 (Invitrogen) and glutamine (Invitrogen). Cells were maintained *in vitro* at 37°C in a 5% CO_2-humified incubator.

Hydrogen peroxide treatment - Primary hippocampal neurons were infected on DIV3 with CDKL5-Flag (ad-CDKL5) or GFP (ad-GFP) adenovirus particles (Vector BioLabs) at 100 multiplicities of infection (MOI). On DIV10 some primary hippocampal neurons were exposed for 18 h to 100 µM H_2O_2. Cell cultures were fixed in absolute methanol at –20°C for 7 min and processed for immunocytochemistry analysis.

Immunocytochemistry

For BrdU analyses cells were incubated for 6 h with BrdU (10 µM; Sigma-Aldrich), fixed in a 4% paraformaldehyde solution at 37°C for 30 min and processed for BrdU immunocytochemistry

as previously described [25]. For γH2AX analyses cells were fixed in absolute methanol at -20°C for 7 min.

For immunofluorescence studies, the following antibodies were used. Primary antibodies: anti-βIII-tubulin mouse monclonal (TubJ, 1:500, Sigma-Aldrich), anti-phospho histone H3 rabbit polyclonal (pHH3, 1:200, Abcam), anti-BrdU mouse monoclonal (1:200, Roche), anti-cleaved caspase-3 (Asp175) rabbit polyclonal (1:100, Cell Signaling Technology), anti-γH2AX (phospho S139) rabbit polyclonal (1:1000, Abcam), and anti-PARP1 rabbit polyclonal (1:1000, Abcam). Secondary antibodies: Cy3-conjugated anti-mouse antibody (1:200, Jackson Immuno Research Laboratories), Cy3-conjugated anti-rabbit antibody (1:200, Jackson Immuno Research Laboratories), FITC-conjugated anti-mouse antibody (1:200, Jackson Immuno Research) and nuclei were counterstained with Hoechst 33342 (Sigma-Aldrich).

Measurements

Phase contrast or fluorescence images of cells were taken with an Eclipse TE 2000-S microscope (Nikon Instruments Inc.) equipped with a DS-Qi2 digital SLR camera (Nikon Instruments Inc.). Images were taken from random microscopic fields (10 for each coverslip).

Analysis of neurite outgrowth - Neurite outgrowth was measured using the image analysis system Image Pro Plus (Media Cybernetics). Only cells with neurites longer than one cell body diameter were considered as neurite-bearing cells. All experiments were performed at least three times. In each experiment a total of 900 cells were analyzed. The total length of neurites was divided by the total number of cells counted in the areas.

Apoptotic cell death - To assess apoptotic cell death cultures were fixed in a 4% paraformaldehyde solution at 37°C for 30 min and nuclei were stained with Hoechst 33342 (Sigma-Aldrich). Some cultures were stained with anti-cleaved caspase-3 antibody (rabbit polyclonal anti-cleaved

caspase-3 Ab, 1:200, Cell Signaling). Detection was performed using a Cy3-conjugated anti-rabbit IgG (1:200, Jackson Immunoresearch) antibody. Apoptotic cell death was assessed by manually counting the number of pycnotic nuclei or cleaved caspase-3 positive neurons and expressed as a percentage of the total number of cells.

γH2AX intensity - Primary hippocampal neurons were fixed at DIV8 and immunostaining was performed using the following primary antibodies: anti-γH2AX (phospho S139) rabbit polyclonal (1:1000, Abcam) and anti-α-tubulin mouse monoclonal (1:500, Sigma-Aldrich). Detection was performed using a Cy3-conjugated anti-mouse IgG (1:200, Jackson Immunoresearch) and a FITC-conjugated anti-rabbit IgG (1:200, Jackson Immunoresearch) antibody. Nuclei were counterstained with Hoechst-33342 and fluorescence images were acquired at the same intensity. To assess γH2AX nuclear intensity Hoechst and γH2AX images of neurons were processed. The perimeter of the nucleus was traced using the Hoechst counterstaining as a guide to define the nuclear area of each cell, and the intensity of Cy3-staining corresponding to the γH2AX signal was quantified by determining the number of positive (bright) pixels within the nucleus.

γH2AX foci per cell – γH2AX automatic foci counting was performed on fluorescence images using the Automatic Bright Objects Count/Size tool in Image Pro Plus (Media Cybernetics). Foci number per image was divided by total cell number. In each condition a total of 2000 cells were analysed.

Western blotting

For the preparation of total cell extracts, cells were lysed in RIPA buffer (50 mM Tris–HCl, pH 7.4, 150 mM NaCl, 1% Triton-X100, 0.5% sodium deoxycholate, 0.1% SDS) supplemented with 1 mM PMSF and 1% protease and phosphatase inhibitor cocktail (Sigma-Aldrich). Protein concentration was determined using the Lowry method [26]. For the preparation of total cell extracts for the evaluation of DNA damage-associated biomarkers (i.e. γH2AX, RAD50 and PARP1),

cells were lysed in lysis buffer containing 20 mM Tris-HCl, pH 7.5, 1% SDS, 1 mM Na3VO4, 1 mM PMSF, 5% β-mercaptoethanol, and protease inhibitors (Sigma-Aldrich). Protein concentration was determined using the Bradford method [27].

Equivalent amounts (50 μg) of protein were subjected to electrophoresis on a 4–12% Mini-PROTEAN® TGX™ Gel (Bio-Rad) and transferred to a Hybond ECL nitrocellulose membrane (GE Healthcare Bio-Science). The following primary antibodies were used: rabbit polyclonal anti-GAPDH (1:5000, Sigma-Aldrich), rabbit polyclonal anti-CDKL5 (1:1000, Sigma-Aldrich), rabbit polyclonal anti-phospho-ERK1/2-Thr202/Tyr204 (1:1000, Cell Signaling Technology), mouse monoclonal anti-ERK1/2 (1:1000, Cell Signaling Technology), rabbit polyclonal anti-phospho-AKT-Ser473 (1:1000, Cell Signaling Technology), rabbit polyclonal anti-AKT (1:1000, Cell Signaling Technology), rabbit polyclonal antiphospho-GSK3β-Ser9 (1:1000, Cell Signaling Technology), rabbit polyclonal anti-GSK3β (1:1000, Cell Signaling Technology), rabbit polyclonal anti-phospho-p90RSK-Ser380 (1:1000, Cell Signaling Technology), rabbit polyclonal anti-phospho-PDK1 (1:1000, Cell Signaling Technology), rabbit polyclonal anti-Bax (1:1000, Cell Signaling Technology), rabbit polyclonal anti-phospho-γH2AX-Ser139 (1:1000, Abcam), rabbit polyclonal anti-RAD50 (1:1000, Elabscience), and rabbit polyclonal anti-PARP1 (1:1000, Abcam). The secondary antibodies used were as follows: HRP-conjugated goat anti-rabbit IgG and HRP-conjugated goat anti-mouse IgG (Jackson Immuno Research) antibodies diluted 1:5000. Densitometric analysis of digitized images was performed using Chemidoc XRS Imaging Systems and Image LabTM Software (Bio-Rad).

In vivo experimental protocol

KA treatment- Experiments were carried out on a total of 12 *Cdkl5* -/Y and 10 *Cdkl5* +/Y mice. Seizures were induced in 10-12-week-old mice by intraperitoneal administration of 25 mg/kg

kainic acid (KA; Sigma-Aldrich) in phosphate-buffered saline (PBS). Seizure grades were scored according to [28] and recorded in a 120-min observation period.

Immunohistochemical and histological procedures - For cell density experiments animals were deeply anesthetized with isoflurane (4% in pure oxygen) and sacrificed by cervical dislocation. Brains were quickly removed, cut along the midline and hemispheres were fixed by immersion in 4% paraformaldehyde in 100 mM phosphate buffer, pH 7.4. Brains were stored in fixative solution for 48 h, kept in 20% sucrose in phosphate buffer for an additional 24 h and then frozen with cold ice. Brains were cut with a freezing microtome into 30-µm-thick coronal sections that were serially collected. Hoechst 33342 staining was used to identify cell nuclei. Hoechst 33342-positive cells were manually counted using the point tool in Image Pro Plus (Media Cybernetics) in one out of 6 sections of the hippocampal formation. The density of cell nuclei in CA1 and CA3 was established as cells/mm^3.

For γH2AX-immunolabeling experiments animals were deeply anesthetized with isoflurane (4% in pure oxygen) and sacrificed by cervical dislocation. Brains were quickly removed, cut along the midline and the hemispheres were fixed by immersion in Glyo-Fix (Thermo Electron Corp.) for 24 h and embedded in paraffin. The forebrain was coronally sectioned into 8 µm thick sections that were attached to poly-lysine-coated slides. One out of 12 sections from the hippocampal formation was stained using a rabbit polyclonal anti-phospho-γH2AX-Ser139 (1:1000, Abcam) antibody. Sections were retrieved with citrate buffer (pH 6.0) at 98°C for 40 min before incubation with the antibody and were processed as previously described [29]. Sections were incubated with Cy3-conjugated anti-rabbit (1:200; Jackson Immuno Research) secondary antibody. Fluorescent images were acquired using a Nikon Eclipse TE600 microscope equipped with a Nikon Digital Camera DXM1200 ATI System (Nikon Instruments Inc.). The analysis of nuclear γH2AX intensity was performed under constant microscope settings. The perimeter of the nucleus was traced

using Hoechst counterstaining as a guide to define the nuclear area of each cell, and the intensity of Cy3 staining corresponding to the γH2AX signal was quantified by determining the number of positive (bright) pixels within the nucleus.

Statistical analysis

Values are expressed as means ± standard error (SEM). The significance of results was obtained using Student's t test and one-way or two-way ANOVA followed by Fisher's LSD post-hoc test. A probability level of $P< 0.05$ was considered to be statistically significant.

RESULTS

Human cellular model of CDKL5 deficiency shows reduced neuronal maturation

To create a human neuronal cell model of CDKL5 deficiency, we generated CRISPR-induced CDKL5 knockout (KO) clones of the human neuroblastoma SH-SY5Y cell line, a well-characterized *in vitro* model of neuronal function and maturation [30-33]. CDKL5 knockout (KO) SH-SY5Y neuroblastoma cell lines (SH-CDKL5-KO) were screened for the absence of CDKL5 expression by Western blot analysis (Fig. 1A). Among the multiple independent SH-CDKL5-KO clones that were negative for CDKL5 protein expression, clones SH-CDKL5-KO1 and SH-CDKL5-KO2 were chosen for further analysis.

Given the known role of CDKL5 in neuronal maturation [16,34,24,17], we first evaluated the effect of CDKL5 depletion in SH-SY5Y neuronal differentiation. In agreement with previous reports [30], when SH-SY5Y cells were treated with retinoic acid (RA) for 5 days (Fig. 1B), a considerable proportion of cells differentiated to a more neuronal phenotype by extending

neuritic processes (Fig. 1C,D). RA-treated SH-CDKL5-KO clones showed reduced neurite outgrowth in comparison with parental cells (Fig. 1C,D). CDKL5 re-expression restored neuritic length in SH-CDKL5-KO clones (Fig. 1C), confirming that defective neuronal differentiation was due to CDKL5 deficiency. No effect of CDKL5 overexpression on neuritic process outgrowth was evident in parental cells (Fig. 1C), probably due to the already strong up-regulation of endogenous CDKL5 expression in differentiating SH-SY5Y cells [35]. It has been reported that RA treatment induces the expression of functional TrkB receptor in SH-SY5Y cells, making them responsive to BDNF [36]. The sequential treatment of SH-SY5Y cells with RA and BDNF (Fig. 1B) was used to support further SH-SY5Y neuronal differentiation, leading to a mature neuronal phenotype, characterized by neurites with several varicosities, also known as “en passant” synapses [36,30,37]. Compared to parental cells, differentiated SH-CDKL5-KO clones were characterized by a remarkable reduction in neurite outgrowth (Fig. 1E,F) and in the number of neurite varicosities (Fig. 1E,F), highly reminiscent of deficits in neuronal maturation (e.g., dendritic morphogenesis and synapse development) previously observed in animal models of CDD [15,24,34,11].

Human cellular model of CDKL5 deficiency exhibits alterations in AKT and ERK signalling pathways

AKT and ERK signalling pathways are critical modulators of a variety of physiological neuronal processes, including differentiation [38,39]. We examined whether these pathways, known to be altered in the brain of *Cdkl5* KO mice [40,41,16,34,11,12], were similarly affected in SH-CDKL5-KO clones. An outline of key elements of the pathways is reported in Fig. 2A. Decreased levels of phosphorylated extracellular signal-regulated kinases (ERK1/2), p90 ribosomal S6 kinase (p90RSK), phosphoinositide-dependent kinase-1 (PDK1), AKT and glycogen synthase kinase 3β

kinase (GSK3β) were observed in extracts of SH-CDKL5-KO cells, when compared to parental SH-SY5Y cells (Fig. 2B,C).

Human cellular model of CDKL5 deficiency exhibits reduced proliferation and survival

To investigate the consequences of CDKL5 depletion on other fundamental cellular functions, we analysed SH-CDKL5-KO cell proliferation and survival. The growth curve of SH-CDKL5-KO cells, monitored over 48 h, showed a reduced growth behaviour of both SH-CDKL5-KO clones in comparison with parental SH-SY5Y cells (−28%; Fig. 3A), suggesting a proliferation and/or survival defect of SH-CDKL5-KO cells. Reduced proliferation was confirmed by a reduced BrdU incorporation rate of SH-CDKL5-KO1 cells versus parental cells (−27%; Fig. 3B,C). Immunocytochemistry for phosphorylated-(Ser10)-histone-H3 (pHH3) allows for the discrimination of cells in the G2 or M phases of the cell cycle [42]. Cells in G2 exhibit punctate pHH3 nuclear staining, which turns to a homogeneously condensed pattern once they enter the M phase (Fig. 3E). As shown in Fig. 3D the percentage of SH-CDKL5-KO1 cells in the G2 or M phases of the cell cycle was reduced compared to parental cells. Restoration of CDKL5 expression normalized the proliferation rate of SH-CDKL5-KO cells (Fig. 3B-E).

To investigate cell viability in SH-CDKL5-KO clones, we evaluated the percentage of pyknotic nuclei in proliferating or RA-induced differentiating cells. We observed an increase in the fraction of pyknotic nuclei in both proliferating and differentiating SH-CDKL5-KO clones compared to the parental cells (Fig. 4A,B). Interestingly, the increased cell death was exacerbated in SH-CDKL5-KO clones during the neuronal differentiation process (Fig. 4A,B). As expected, re-expression of CDKL5 restored cell survival in SH-CDKL5-KO cells (Fig. 4C). Increased apoptosis in CDKL5 deficient cells was confirmed by the increased percentage of cleaved caspase-3 positive cells in SH-CDKL5-KO1 cells in comparison with parental cells (Fig. 4D,E), and by the increased expression of the pro-apoptotic Bcl-2-associated X protein (BAX; Fig. 4F,G). In agreement with the

increased cell death during RA-induced differentiation (Fig. 3A), differentiating SH-CDKL5-KO1 cells show higher levels of BAX protein (Fig. 4F,G).

Human cellular model of CDKL5 deficiency shows increased levels of biological markers associated with DNA damage

Cell cycle progression and apoptosis are finely regulated processes that serve to determine the fate of cells in response to various stresses; one such stress is DNA damage. When the DNA damage is too severe or there are defects in the DNA repair system, cells can undergo permanent cell-cycle arrest or cell death [43]. When cells sustain a DNA double-strand break (DSB), histone H2AX in chromatin surrounding the DNA break is phosphorylated, marking repair foci. The number of phosphorylated histone H2AX (γH2AX) foci approximates the number of DSBs present in the cell's nuclear DNA [44]. γH2AX promotes recruitment of DNA damage response (DDR) proteins, including the MRN (MRE11–RAD50–NBS1) complex [45]. To explore the possibility that reduced cell cycle progression and survival in SH-CDKL5-KO cells might underlie a defect in the DNA repair process, we analysed the levels of γH2AX and RAD50 proteins and the number of foci/cell of γH2AX in SH-CDKL5-KO cells. As shown by Western blot (Fig. 5A,B) and immunocytochemistry (Fig. 5D,E), γH2AX levels and foci number were significantly higher in SH-CDKL5-KO clones compared to parental cells; accordingly, we also found increased RAD50 levels (Fig. 5A,B). Re-expression of CDKL5 reduced γH2AX levels and foci number in SH-CDKL5-KO1 cells at the level of parental cells (Fig. 5C-E). In agreement with the increased apoptotic cell death during RA-induced differentiation (Fig. 4A,B), differentiating SH-CDKL5-KO1 cells showed higher levels of γH2AX and RAD50 compared to parental cells (Supplementary Fig. 1A,B).

Poly(ADP-ribose) polymerase-1 (PARP-1), which is an enzyme that participates in the repair of many forms of DNA damage [46-48], delocalized from the nucleolus in cells exposed to DNA-

damaging agents [49,50]. While no difference in PARP1 levels were observed between SH-CDKL5-KO and parental cells (Fig. 5A,B), a delocalization of PARP-1 from the nucleolus to the nucleoplasm was clearly present in SH-CDKL5-KO cells (Fig. 5F), indicating a cellular response to DNA damage.

Increased stress-induced DNA damage in CDKL5-null neurons

The DNA damage response in CDKL5-deficient cells could result from failure to repair DNA damage caused by oxidative stress occurring under standard culture conditions [51]. A recent study indicated that *Cdkl5* KO hippocampal neurons are more vulnerable to excitotoxicity, metabolic, and oxidative stress [23], all conditions that damage DNA [52-56]. To test whether CDKL5 was indeed required for a proper cellular response to such damage, we examined the viability and the DNA damage induction of SH-CDKL5-KO cells after oxidative (H_2O_2) and metabolic stress (serum starvation). SH-CDKL5-KO cells were more sensitive to treatment with H_2O_2 and serum withdrawal than parental SH-SY5Y cells (Fig. 6A-C). In parallel, γH2AX levels and foci number were significantly higher in H_2O_2-treated SH-CDKL5-KO clones compared to parental cells (Fig. 6D-F).

Similarly to SH-CDKL5-KO1 cells, hippocampal *Cdkl5* -/Y neurons showed an increased γH2AX nuclear staining in comparison with wild-type neurons (+/Y) (Fig. 7A,C). In agreement with the increased neuronal vulnerability of *Cdkl5* -/Y neurons to H_2O_2-induced apoptosis [23], treatment with H_2O_2 induced a higher increase in DNA damage response (γH2AX staining) in *Cdkl5* -/Y neurons in comparison with wild-type neurons (+/Y) (Fig. 7A). Importantly, the re-expression of CDKL5 restored γH2AX staining in hippocampal cultures from *Cdkl5* -/Y mice (Fig. 7B,C).

Increased DNA damage after KA-induced cell death in hippocampal neurons from *Cdkl5* KO mice

To determine whether, also *in vivo, Cdkl5* KO neurons show an increase in the DNA-damage response after excitotoxic stimuli, we intraperitoneally injected *Cdkl5* -/Y and wild-type (+/Y) mice with kainic acid (KA; 25 mg/kg). No difference in seizure intensity was observed between *Cdkl5* -/Y and wild-type (+/Y) mice in the 120 minutes following KA administration (Fig. 8A)**.** In the CA3 and CA1 layers of the hippocampus, 8 days after KA injection, *Cdkl5* -/Y mice showed a lower cell density in comparison with wild-type mice (Fig. 8B,C), indicating that *Cdkl5* -/Y mice are more vulnerable to neurotoxicity induced by treatment with KA. Interestingly, KA-treated *Cdkl5* -/Y mice showed an increased γH2AX immunostaining in comparison with wild-type mice (+/Y) (Fig. 8D,E), indicating an increased DNA damage in the absence of CDKL5 after excitotoxic stimuli.

DISCUSSION

In order to develop an effective therapy for CDD, improvement of our current understanding of the molecular and cellular mechanisms underlying CDD pathogenesis is crucial. For this purpose, the development of human cellular models of the disease is necessary. In this study, we generated a model of CDKL5 deficiency, starting from the human neuroblastoma cell line, SH-SY5Y. We chose this cell line because of its human origin and neuronal properties. We demonstrated that the SH-SY5Y cell line, similar to those observed *in vivo* during brain development [57,5], exhibits a positive correlation between CDKL5 expression and neuronal differentiation [35], indicating that this human cell line may represent a suitable model with which to study the role of CDKL5 in neurons. Importantly, characterization of CDKL5-deficient SH-SY5Y cells uncovered a new, previously undescribed, role of CDKL5 in the process of DNA damage

response. These findings provide novel evidence concerning the complex, multifaceted role of CDKL5 in maintaining the proper balance between cell differentiation, survival, and DNA repair processes in neuronal cells.

The human cellular model of CDKL5 deficiency recapitulates deficits in neuronal maturation and alterations in signalling pathways previously described in *Cdkl5* KO mice

We provide evidence that CDKL5 deficiency in the SH-SY5Y neuroblastoma cell line impaired proper neurite outgrowth during neuronal differentiation. This is consistent with a body of evidence in *Cdkl5* KO mice, showing that CDKL5 regulates neurite growth and dendritic arborization of cortical and hippocampal neurons [15,34,11,18]. Furthermore, the inability of SH-CDKL5-KO cells to produce a proper number of neuritic varicosities, highly specialized compartments that serve as functional sites for neurotransmitter release, confirms previous evidence that CDKL5-null neurons are characterized by impaired synaptogenesis [17,24,19]. Our data provide further compelling evidence as to the key role that CDKL5 plays in proper dendritic morphogenesis and synapse development and validate SH-CDKL5 KO cells as a reliable cellular model for the study of CDKL5 functions in a cellular context.

AKT and ERK signalling pathways are crucial for neuronal functions that regulate neurogenesis, neuron survival and differentiation, and synaptic plasticity, as well as memory formation, and the alterations of these pathways can contribute to the progression of neurological diseases in various conditions [58,38,39]. Our finding that AKT and ERK signalling pathways are altered in SH-CDKL5 KO cells is in line with previous evidence in two independent animal models for CDD [12,15,34,11], and strongly suggests that loss of CDKL5 activity affects neuronal maturation/function by impairing AKT and ERK signalling pathways.

Impaired cell proliferation, survival and DNA damage response in a human cellular model of CDKL5 deficiency

Our finding that CDKL5 deficiency in SH-CDKL5-KO cells results in a decrease in cell proliferation and in an increase in cell death may be ascribable to the observed deregulation of AKT and ERK signalling pathways, critical modulators of a variety of physiological processes including proliferation and apoptosis [38,39]. However, the increased levels of DNA repair biomarkers in SH-CDKL5-KO cells, an index of increased DNA damage, suggests that CDKL5 contributes to DNA repair processes and thereby controls the fine balance between cell cycle progression and apoptosis. Indeed, in eukaryotic cells, control mechanisms have been developed that restrain cell-cycle transitions in response to stress termed cell-cycle checkpoints [59]. These mechanisms prevent cells from proceeding in the cell cycle when DNA is damaged in order to afford these cells an opportunity to repair the damaged DNA before propagating genetic defects to the daughter cells. If the damage is irreparable, checkpoint signalling might activate pathways that lead to apoptosis [43,60]. A connection between DNA damage and apoptosis in CDKL5-null cells is supported by our finding that SH-CDKL5-KO cells express high levels of the pro-apoptotic BAX (Bcl2-associated X) protein, a key mediator of the apoptotic response to DNA damage [61].

Previous studies in SH-SY5Y neuroblastoma cells and in *Cdkl5* KO mice suggested that CDKL5 inhibits cell proliferation [35,34]. However, in the postnatal developing mouse hippocampus, genetic inactivation of *Cdkl5* increases the proliferation rate of IPCs but causes the death of immature newborn neurons, thereby modulating the intricate balance between precursor proliferation and survival. In agreement with a recent observation in HeLa cells, in which CDKL5 loss-of-function correlates with an impaired cell division [62], our results suggest that the influence of CDKL5 on cell fate (proliferation/survival) might be linked to its effects on genome stability.

Increased stress-induced DNA damage in CDKL5-null neurons

The increased susceptibility of SH-CDKL5-KO cells to oxidative stress further demonstrates that *Cdkl5*-null neurons are more vulnerable to excitotoxicity, metabolic, and oxidative stress [23]. Our finding that, in the absence of CDKL5, the increased neuronal susceptibility to neurotoxic stress is paralleled by an increased DNA damage response corroborates the hypothesis that CDKL5 deficient cells fail to repair DNA damage. DNA damage is countered by a complex defence mechanism, which involves many proteins including kinases [63]. Although we do not currently know how CDKL5 contributes to the complex mechanism of DNA repair, its nuclear localization at the centrosome [62], a critical cellular organelle that integrates signals in response to DNA damage, together with the high levels of the DNA damage biomarker γH2AX in CDKL5-null neurons, strongly suggests that CDKL5 contributes to DNA repair. Moreover, the increased vulnerability of hippocampal neurons observed in response to KA treatment in *Cdkl5* KO mice can be ascribable to increased DNA damage. Systemic administration of KA to rodents results in neuronal damage associated with DNA strand breaks in the hippocampus of p53-deficient mice [64], suggesting that the functionality of the DNA repair machinery allows hippocampal neurons to recover from KA-induced DNA damage. Increased DNA biomarkers in *Cdkl5* KO hippocampal neurons is an index of decreased DNA repair capacity, which may justify the reduced neuronal survival.

Conclusions

Insufficiency in DNA repair is a mechanism that can precipitate DNA damage, and it has been implicated in the pathogenesis of many neurologic disorders, including neurodevelopmental disorders [65]. Indeed, several studies have linked polymorphisms in DNA repair genes to the

development of schizophrenia and autism [66]. Moreover, defects in the kinases DNA-PKcs, ATM, and ATR, central regulators of DNA repair, have been linked to neurodegenerative or neurodevelopmental disorders [63]. Understanding whether altered DNA repair and/or DNA damage play a role in the pathophysiology of CDD will provide a rational basis for therapies targeted at ameliorating the neurological problems in this syndrome.

ACKNOWLEDGMENTS

This work was supported by the Italian parent association “CDKL5 insieme verso la cura”.

DISCLOSURE

All authors report that they have no biomedical financial interests or potential conflicts of interest.

BIBLIOGRAPHY

1. Fehr S, Wilson M, Downs J, Williams S, Murgia A, Sartori S, Vecchi M, Ho G, Polli R, Psoni S, Bao X, de Klerk N, Leonard H, Christodoulou J (2013) The CDKL5 disorder is an independent clinical entity associated with early-onset encephalopathy. Eur J Hum Genet 21 (3):266-273. doi:10.1038/ejhg.2012.156

2. Dale T, Downs J, Olson H, Bergin AM, Smith S, Leonard H (2019) Cannabis for refractory epilepsy in children: A review focusing on CDKL5 Deficiency Disorder. Epilepsy Res 151:31-39. doi:10.1016/j.eplepsyres.2019.02.001

3. Montini E, Andolfi G, Caruso A, Buchner G, Walpole SM, Mariani M, Consalez G, Trump D, Ballabio A, Franco B (1998) Identification and characterization of a novel serine-threonine kinase gene from the Xp22 region. Genomics 51 (3):427-433. doi:10.1006/geno.1998.5391

4. Lin C, Franco B, Rosner MR (2005) CDKL5/Stk9 kinase inactivation is associated with neuronal developmental disorders. Hum Mol Genet 14 (24):3775-3786. doi:10.1093/hmg/ddi391

5. Rusconi L, Salvatoni L, Giudici L, Bertani I, Kilstrup-Nielsen C, Broccoli V, Landsberger N (2008) CDKL5 expression is modulated during neuronal development and its subcellular distribution is tightly regulated by the C-terminal tail. J Biol Chem 283 (44):30101-30111. doi:10.1074/jbc.M804613200

6. Bahi-Buisson N, Bienvenu T (2012) CDKL5-Related Disorders: From Clinical Description to Molecular Genetics. Mol Syndromol 2 (3-5):137-152. doi:000331333

7. Fehr S, Downs J, Ho G, de Klerk N, Forbes D, Christodoulou J, Williams S, Leonard H (2016) Functional abilities in children and adults with the CDKL5 disorder. Am J Med Genet A 170 (11):2860-2869. doi:10.1002/ajmg.a.37851

8. Fehr S, Wong K, Chin R, Williams S, de Klerk N, Forbes D, Krishnaraj R, Christodoulou J, Downs J, Leonard H (2016) Seizure variables and their relationship to genotype and functional abilities in the CDKL5 disorder. Neurology 87 (21):2206-2213. doi:10.1212/WNL.0000000000003352

9. Neupauerova J, Sterbova K, Vlckova M, Sebronova V, Marikova T, Krutova M, David S, Krsek P, Zaliova M, Seeman P, Lassuthova P (2017) Two Novel Variants Affecting CDKL5 Transcript Associated with Epileptic Encephalopathy. Genet Test Mol Biomarkers 21 (10):613-618. doi:10.1089/gtmb.2017.0110

10. Kilstrup-Nielsen C, Rusconi L, La Montanara P, Ciceri D, Bergo A, Bedogni F, Landsberger N (2012) What we know and would like to know about CDKL5 and its involvement in epileptic encephalopathy. Neural Plast 2012:728267. doi:10.1155/2012/728267

11. Amendola E, Zhan Y, Mattucci C, Castroflorio E, Calcagno E, Fuchs C, Lonetti G, Silingardi D, Vyssotski AL, Farley D, Ciani E, Pizzorusso T, Giustetto M, Gross CT (2014) Mapping pathological phenotypes in a mouse model of CDKL5 disorder. PLoS One 9 (5):e91613. doi:10.1371/journal.pone.0091613

12. Wang IT, Allen M, Goffin D, Zhu X, Fairless AH, Brodkin ES, Siegel SJ, Marsh ED, Blendy JA, Zhou Z (2012) Loss of CDKL5 disrupts kinome profile and event-related potentials leading to autistic-like phenotypes in mice. Proc Natl Acad Sci U S A 109 (52):21516-21521. doi:10.1073/pnas.1216988110

13. Tang S, Wang IJ, Yue C, Takano H, Terzic B, Pance K, Lee JY, Cui Y, Coulter DA, Zhou Z (2017) Loss of CDKL5 in Glutamatergic Neurons Disrupts Hippocampal Microcircuitry and Leads to Memory Impairment in Mice. J Neurosci 37 (31):7420-7437. doi:10.1523/JNEUROSCI.0539-17.2017

14. Okuda K, Takao K, Watanabe A, Miyakawa T, Mizuguchi M, Tanaka T (2018) Comprehensive behavioral analysis of the Cdkl5 knockout mice revealed significant enhancement in anxiety- and

fear-related behaviors and impairment in both acquisition and long-term retention of spatial reference memory. PLoS One 13 (4):e0196587. doi:10.1371/journal.pone.0196587

15. Fuchs C, Gennaccaro L, Trazzi S, Bastianini S, Bettini S, Martire VL, Ren E, Medici G, Zoccoli G, Rimondini R, Ciani E (2018) Heterozygous CDKL5 Knockout Female Mice Are a Valuable Animal Model for CDKL5 Disorder. Neural Plast 2018:9726950. doi:10.1155/2018/9726950

16. Fuchs C, Rimondini R, Viggiano R, Trazzi S, De Franceschi M, Bartesaghi R, Ciani E (2015) Inhibition of GSK3beta rescues hippocampal development and learning in a mouse model of CDKL5 disorder. Neurobiol Dis 82:298-310. doi:10.1016/j.nbd.2015.06.018

17. Della Sala G, Putignano E, Chelini G, Melani R, Calcagno E, Michele Ratto G, Amendola E, Gross CT, Giustetto M, Pizzorusso T (2016) Dendritic Spine Instability in a Mouse Model of CDKL5 Disorder Is Rescued by Insulin-like Growth Factor 1. Biol Psychiatry 80 (4):302-311. doi:10.1016/j.biopsych.2015.08.028

18. Ren E, Roncacé V, Trazzi S, Fuchs C, Medici G, Gennaccaro L, Loi M, Galvani G, Ye K, Rimondini R, Aicardi G, Ciani E (2019) Functional and Structural Impairments in the Perirhinal Cortex of a Mouse Model of CDKL5 Deficiency Disorder Are Rescued by a TrkB Agonist. Frontiers in Cellular Neuroscience 13 (169). doi:10.3389/fncel.2019.00169

19. Pizzo R, Gurgone A, Castroflorio E, Amendola E, Gross C, Sassoe-Pognetto M, Giustetto M (2016) Lack of Cdkl5 Disrupts the Organization of Excitatory and Inhibitory Synapses and Parvalbumin Interneurons in the Primary Visual Cortex. Front Cell Neurosci 10:261. doi:10.3389/fncel.2016.00261

20. Ricciardi S, Ungaro F, Hambrock M, Rademacher N, Stefanelli G, Brambilla D, Sessa A, Magagnotti C, Bachi A, Giarda E, Verpelli C, Kilstrup-Nielsen C, Sala C, Kalscheuer VM, Broccoli V (2012) CDKL5 ensures excitatory synapse stability by reinforcing NGL-1-PSD95 interaction in the

postsynaptic compartment and is impaired in patient iPSC-derived neurons. Nat Cell Biol 14 (9):911-923. doi:10.1038/ncb2566

21. Trazzi S, De Franceschi M, Fuchs C, Bastianini S, Viggiano R, Lupori L, Mazziotti R, Medici G, Lo Martire V, Ren E, Rimondini R, Zoccoli G, Bartesaghi R, Pizzorusso T, Ciani E (2018) CDKL5 protein substitution therapy rescues neurological phenotypes of a mouse model of CDKL5 disorder. Hum Mol Genet 27 (9):1572-1592. doi:10.1093/hmg/ddy064

22. Zhu YC, Xiong ZQ (2019) Molecular and Synaptic Bases of CDKL5 Disorder. Dev Neurobiol 79 (1):8-19. doi:10.1002/dneu.22639

23. Fuchs C, Medici G, Trazzi S, Gennaccaro L, Galvani G, Berteotti C, Ren E, Loi M, Ciani E (2019) CDKL5 deficiency predisposes neurons to cell death through the deregulation of SMAD3 signaling. Brain Pathol. doi:10.1111/bpa.12716

24. Trazzi S, Fuchs C, Viggiano R, De Franceschi M, Valli E, Jedynak P, Hansen FK, Perini G, Rimondini R, Kurz T, Bartesaghi R, Ciani E (2016) HDAC4: a key factor underlying brain developmental alterations in CDKL5 disorder. Hum Mol Genet 25 (18):3887-3907. doi:10.1093/hmg/ddw231

25. Contestabile A, Fila T, Cappellini A, Bartesaghi R, Ciani E (2009) Widespread impairment of cell proliferation in the neonate Ts65Dn mouse, a model for Down syndrome. Cell Prolif 42 (2):171-181. doi:10.1111/j.1365-2184.2009.00587.x

26. Lowry OH, Rosebrough NJ, Farr AL, Randall RJ (1951) Protein measurement with the Folin phenol reagent. J Biol Chem 193 (1):265-275

27. Bradford MM (1976) A rapid and sensitive method for the quantitation of microgram quantities of protein utilizing the principle of protein-dye binding. Anal Biochem 72:248-254

28. Wu G, Lu ZH, Wang J, Wang Y, Xie X, Meyenhofer MF, Ledeen RW (2005) Enhanced susceptibility to kainate-induced seizures, neuronal apoptosis, and death in mice lacking

gangliotetraose gangliosides: protection with LIGA 20, a membrane-permeant analog of GM1. J Neurosci 25 (47):11014-11022. doi:10.1523/JNEUROSCI.3635-05.2005

29. Contestabile A, Fila T, Ceccarelli C, Bonasoni P, Bonapace L, Santini D, Bartesaghi R, Ciani E (2007) Cell cycle alteration and decreased cell proliferation in the hippocampal dentate gyrus and in the neocortical germinal matrix of fetuses with Down syndrome and in Ts65Dn mice. Hippocampus 17 (8):665-678. doi:10.1002/hipo.20308

30. Encinas M, Iglesias M, Liu Y, Wang H, Muhaisen A, Cena V, Gallego C, Comella JX (2000) Sequential treatment of SH-SY5Y cells with retinoic acid and brain-derived neurotrophic factor gives rise to fully differentiated, neurotrophic factor-dependent, human neuron-like cells. J Neurochem 75 (3):991-1003

31. Christensen J, Steain M, Slobedman B, Abendroth A (2011) Differentiated neuroblastoma cells provide a highly efficient model for studies of productive varicella-zoster virus infection of neuronal cells. J Virol 85 (16):8436-8442. doi:10.1128/JVI.00515-11

32. Gimenez-Cassina A, Lim F, Diaz-Nido J (2006) Differentiation of a human neuroblastoma into neuron-like cells increases their susceptibility to transduction by herpesviral vectors. J Neurosci Res 84 (4):755-767. doi:10.1002/jnr.20976

33. Shipley MM, Mangold CA, Kuny CV, Szpara ML (2017) Differentiated Human SH-SY5Y Cells Provide a Reductionist Model of Herpes Simplex Virus 1 Neurotropism. J Virol 91 (23). doi:10.1128/JVI.00958-17

34. Fuchs C, Trazzi S, Torricella R, Viggiano R, De Franceschi M, Amendola E, Gross C, Calza L, Bartesaghi R, Ciani E (2014) Loss of CDKL5 impairs survival and dendritic growth of newborn neurons by altering AKT/GSK-3beta signaling. Neurobiol Dis 70:53-68. doi:10.1016/j.nbd.2014.06.006

35. Valli E, Trazzi S, Fuchs C, Erriquez D, Bartesaghi R, Perini G, Ciani E (2012) CDKL5, a novel MYCN-repressed gene, blocks cell cycle and promotes differentiation of neuronal cells. Biochim Biophys Acta 1819 (11-12):1173-1185. doi:10.1016/j.bbagrm.2012.08.001

36. Kaplan DR, Matsumoto K, Lucarelli E, Thiele CJ (1993) Induction of TrkB by retinoic acid mediates biologic responsiveness to BDNF and differentiation of human neuroblastoma cells. Eukaryotic Signal Transduction Group. Neuron 11 (2):321-331

37. Ferrari-Toninelli G, Bonini SA, Uberti D, Napolitano F, Stante M, Santoro F, Minopoli G, Zambrano N, Russo T, Memo M (2009) Notch activation induces neurite remodeling and functional modifications in SH-SY5Y neuronal cells. Dev Neurobiol 69 (6):378-391. doi:10.1002/dneu.20710

38. Sun Y, Liu WZ, Liu T, Feng X, Yang N, Zhou HF (2015) Signaling pathway of MAPK/ERK in cell proliferation, differentiation, migration, senescence and apoptosis. J Recept Signal Transduct Res 35 (6):600-604. doi:10.3109/10799893.2015.1030412

39. Sanchez-Alegria K, Flores-Leon M, Avila-Munoz E, Rodriguez-Corona N, Arias C (2018) PI3K Signaling in Neurons: A Central Node for the Control of Multiple Functions. Int J Mol Sci 19 (12). doi:10.3390/ijms19123725

40. Fuchs C, Fustini N, Trazzi S, Gennaccaro L, Rimondini R, Ciani E (2018) Treatment with the GSK3-beta inhibitor Tideglusib improves hippocampal development and memory performance in juvenile, but not adult, Cdkl5 knockout mice. Eur J Neurosci 47 (9):1054-1066. doi:10.1111/ejn.13923

41. Fuchs C, Gennaccaro L, Trazzi S, Bastianini S, Bettini S, Lo Martire V, Ren E, Medici G, Zoccoli G, Rimondini R, Ciani E (2018) Heterozygous CDKL5 Knockout Female Mice Are a Valuable Animal Model for CDKL5 Disorder. Neural Plast 2018:9726950. doi:10.1155/2018/9726950

42. Hendzel MJ, Wei Y, Mancini MA, Van Hooser A, Ranalli T, Brinkley BR, Bazett-Jones DP, Allis CD (1997) Mitosis-specific phosphorylation of histone H3 initiates primarily within pericentromeric

heterochromatin during G2 and spreads in an ordered fashion coincident with mitotic chromosome condensation. Chromosoma 106 (6):348-360

43. Fielder E, von Zglinicki T, Jurk D (2017) The DNA Damage Response in Neurons: Die by Apoptosis or Survive in a Senescence-Like State? J Alzheimers Dis 60 (s1):S107-S131. doi:10.3233/JAD-161221

44. Ji J, Zhang Y, Redon CE, Reinhold WC, Chen AP, Fogli LK, Holbeck SL, Parchment RE, Hollingshead M, Tomaszewski JE, Dudon Q, Pommier Y, Doroshow JH, Bonner WM (2017) Phosphorylated fraction of H2AX as a measurement for DNA damage in cancer cells and potential applications of a novel assay. PLoS One 12 (2):e0171582. doi:10.1371/journal.pone.0171582

45. Podhorecka M, Skladanowski A, Bozko P (2010) H2AX Phosphorylation: Its Role in DNA Damage Response and Cancer Therapy. J Nucleic Acids 2010. doi:10.4061/2010/920161

46. Althaus FR, Richter C (1987) ADP-ribosylation of proteins. Enzymology and biological significance. Mol Biol Biochem Biophys 37:1-237

47. Cleaver JE, Morgan WF (1991) Poly(ADP-ribose)polymerase: a perplexing participant in cellular responses to DNA breakage. Mutat Res 257 (1):1-18

48. Lindahl T, Satoh MS, Poirier GG, Klungland A (1995) Post-translational modification of poly(ADP-ribose) polymerase induced by DNA strand breaks. Trends Biochem Sci 20 (10):405-411

49. Rancourt A, Satoh MS (2009) Delocalization of nucleolar poly(ADP-ribose) polymerase-1 to the nucleoplasm and its novel link to cellular sensitivity to DNA damage. DNA Repair (Amst) 8 (3):286-297. doi:10.1016/j.dnarep.2008.11.018

50. Meder VS, Boeglin M, de Murcia G, Schreiber V (2005) PARP-1 and PARP-2 interact with nucleophosmin/B23 and accumulate in transcriptionally active nucleoli. J Cell Sci 118 (Pt 1):211-222. doi:10.1242/jcs.01606

51. Uutela M, Lindholm J, Rantamaki T, Umemori J, Hunter K, Voikar V, Castren ML (2014) Distinctive behavioral and cellular responses to fluoxetine in the mouse model for Fragile X syndrome. Front Cell Neurosci 8:150. doi:10.3389/fncel.2014.00150

52. Murphy TH, Miyamoto M, Sastre A, Schnaar RL, Coyle JT (1989) Glutamate toxicity in a neuronal cell line involves inhibition of cystine transport leading to oxidative stress. Neuron 2 (6):1547-1558

53. Yang JL, Sykora P, Wilson DM, 3rd, Mattson MP, Bohr VA (2011) The excitatory neurotransmitter glutamate stimulates DNA repair to increase neuronal resiliency. Mech Ageing Dev 132 (8-9):405-411. doi:10.1016/j.mad.2011.06.005

54. Narciso L, Parlanti E, Racaniello M, Simonelli V, Cardinale A, Merlo D, Dogliotti E (2016) The Response to Oxidative DNA Damage in Neurons: Mechanisms and Disease. Neural Plast 2016:3619274. doi:10.1155/2016/3619274

55. Altman BJ, Rathmell JC (2012) Metabolic stress in autophagy and cell death pathways. Cold Spring Harb Perspect Biol 4 (9):a008763. doi:10.1101/cshperspect.a008763

56. Liu J, Kim J, Oberdoerffer P (2013) Metabolic modulation of chromatin: implications for DNA repair and genomic integrity. Front Genet 4:182. doi:10.3389/fgene.2013.00182

57. Chen Q, Zhu YC, Yu J, Miao S, Zheng J, Xu L, Zhou Y, Li D, Zhang C, Tao J, Xiong ZQ (2010) CDKL5, a protein associated with rett syndrome, regulates neuronal morphogenesis via Rac1 signaling. J Neurosci 30 (38):12777-12786. doi:10.1523/JNEUROSCI.1102-10.2010

58. Luo J (2012) The role of GSK3beta in the development of the central nervous system. Front Biol 7 (3):212 – 220. doi:DOI 10.1007/s11515-012-1222-2

59. Verma N, Franchitto M, Zonfrilli A, Cialfi S, Palermo R, Talora C (2019) DNA Damage Stress: Cui Prodest? Int J Mol Sci 20 (5). doi:10.3390/ijms20051073

60. Wang JY (2001) DNA damage and apoptosis. Cell Death Differ 8 (11):1047-1048. doi:10.1038/sj.cdd.4400938

61. Zinkel S, Gross A, Yang E (2006) BCL2 family in DNA damage and cell cycle control. Cell Death Differ 13 (8):1351-1359. doi:10.1038/sj.cdd.4401987

62. Barbiero I, Valente D, Chandola C, Magi F, Bergo A, Monteonofrio L, Tramarin M, Fazzari M, Soddu S, Landsberger N, Rinaldo C, Kilstrup-Nielsen C (2017) CDKL5 localizes at the centrosome and midbody and is required for faithful cell division. Sci Rep 7 (1):6228. doi:10.1038/s41598-017-05875-z

63. Enriquez-Rios V, Dumitrache LC, Downing SM, Li Y, Brown EJ, Russell HR, McKinnon PJ (2017) DNA-PKcs, ATM, and ATR Interplay Maintains Genome Integrity during Neurogenesis. J Neurosci 37 (4):893-905. doi:10.1523/JNEUROSCI.4213-15.2016

64. Kinoshita Y, Wenzel HJ, Kinoshita C, Schwartzkroin PA, Morrison RS (2012) Acute, but reversible, kainic acid-induced DNA damage in hippocampal CA1 pyramidal cells of p53-deficient mice. Epilepsia 53 Suppl 1:125-133. doi:10.1111/j.1528-1167.2012.03483.x

65. Youngsoo L, Inseo C, Jusik K, and, Keeeun K (2016) DNA damage to human genetic disorders with neurodevelopmental defects. J Genet Med 13 (1):1-13

66. Markkanen E, Meyer U, Dianov GL (2016) DNA Damage and Repair in Schizophrenia and Autism: Implications for Cancer Comorbidity and Beyond. Int J Mol Sci 17 (6). doi:10.3390/ijms17060856

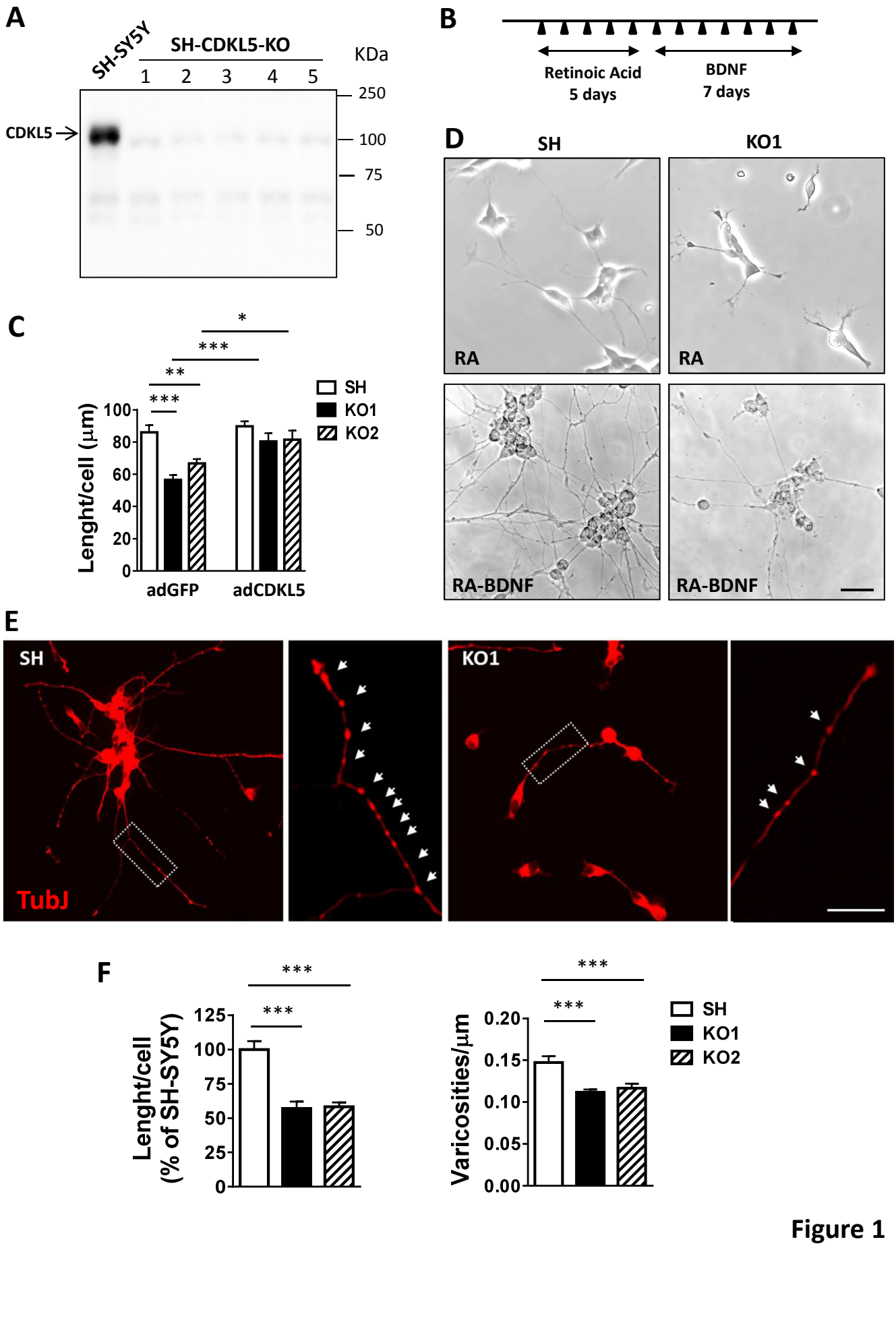
A
SH-SY5Y
SH-CDKL5-KO
KDa
1 2 3 4 5
CDKL5
250
100
75
50
B
Retinoic Acid
5 days
BDNF
7 days
C
*
***
**
***
Lenght/cell (µm)
100
80
60
40
20
0
SH
KO1
KO2
adGFP
adCDKL5
D
SH
KO1
RA
RA
RA-BDNF
RA-BDNF
E
SH
KO1
TubJ
F
***
***
Lenght/cell
(% of SH-SY5Y)
125
100
75
50
25
0
***
***
Varicosities/µm
0.20
0.15
0.10
0.05
0.00
SH
KO1
KO2

Figure 1

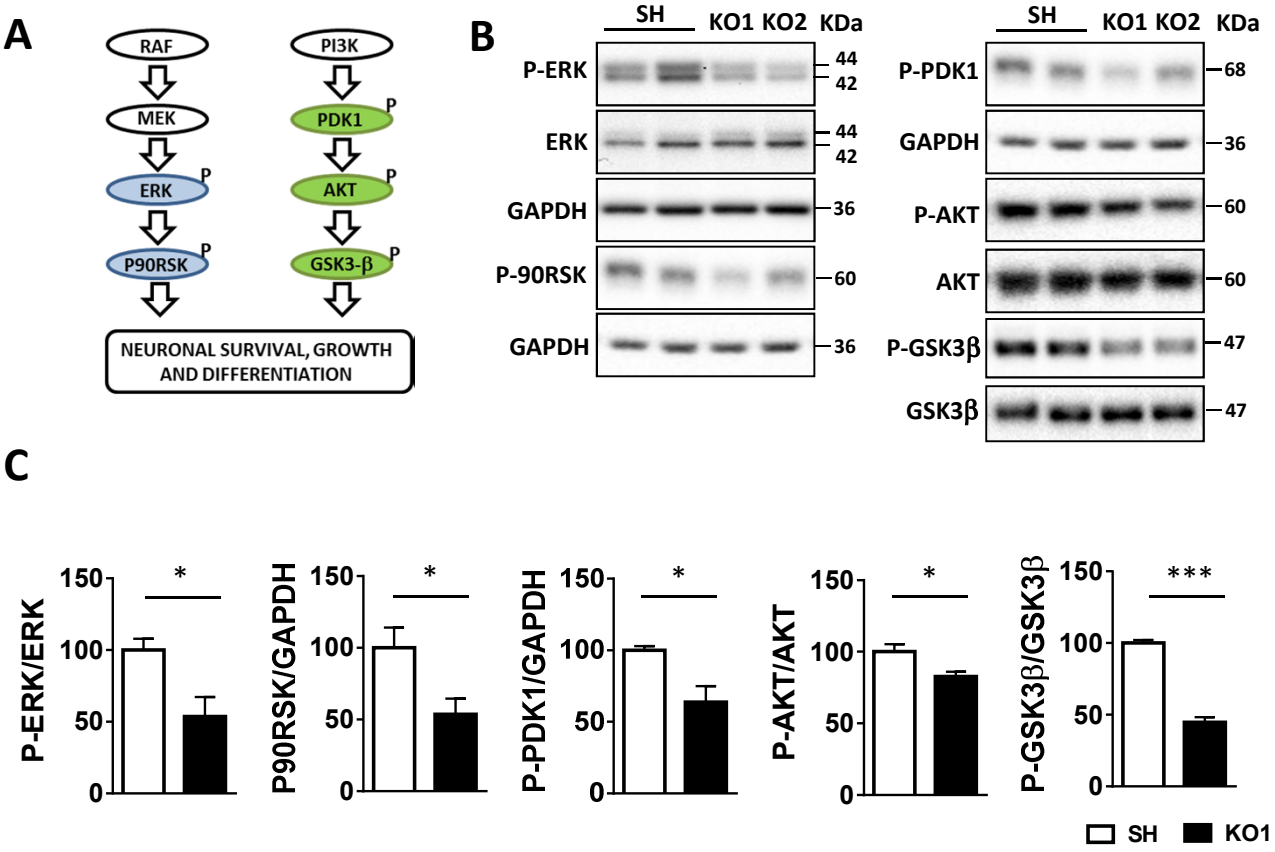
A
RAF
MEK
ERK
P90RSK
PI3K
PDK1
AKT
GSK3-β
P
NEURONAL SURVIVAL, GROWTH AND DIFFERENTIATION
B
SH
KO1 KO2
KDa
P-ERK
ERK
GAPDH
P-90RSK
GAPDH
44
42
44
42
36
60
36
P-PDK1
GAPDH
P-AKT
AKT
P-GSK3β
GSK3β
68
36
60
60
47
47
C
P-ERK/ERK
P90RSK/GAPDH
P-PDK1/GAPDH
P-AKT/AKT
P-GSK3β/GSK3β
150
100
50
0
*
***
SH
KO1

Figure 2

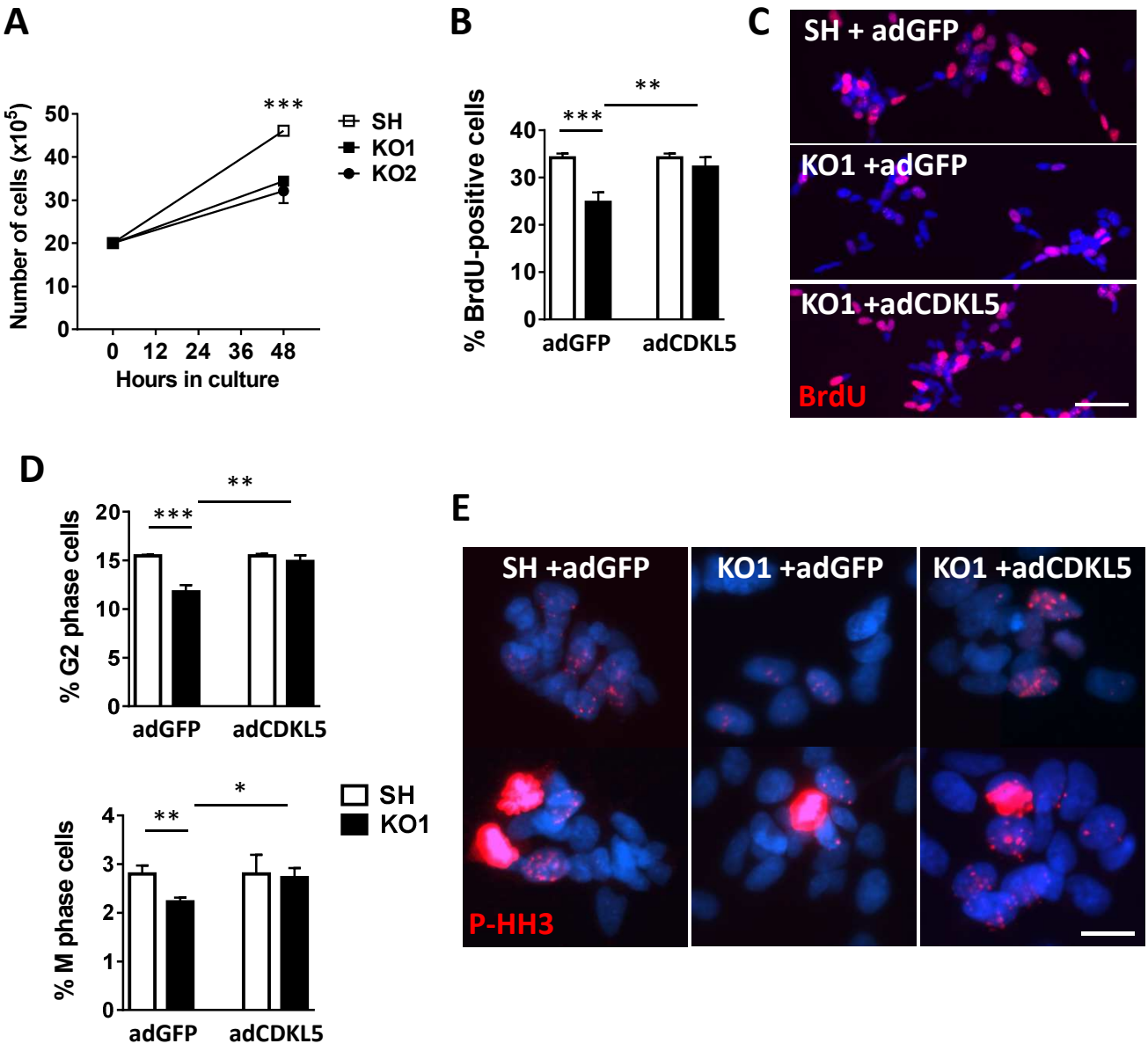
A
Number of cells (x10^5)
50
40
30
20
10
0
0 12 24 36 48
Hours in culture
***
SH
KO1
KO2
B
% BrdU-positive cells
40
30
20
10
0
***
**
adGFP
adCDKL5
C
SH + adGFP
KO1 +adGFP
KO1 +adCDKL5
BrdU
D
% G2 phase cells
20
15
10
5
0
***
**
adGFP
adCDKL5
% M phase cells
4
3
2
1
0
**
*
adGFP
adCDKL5
SH
KO1
E
SH +adGFP
KO1 +adGFP
KO1 +adCDKL5
P-HH3

Figure 3

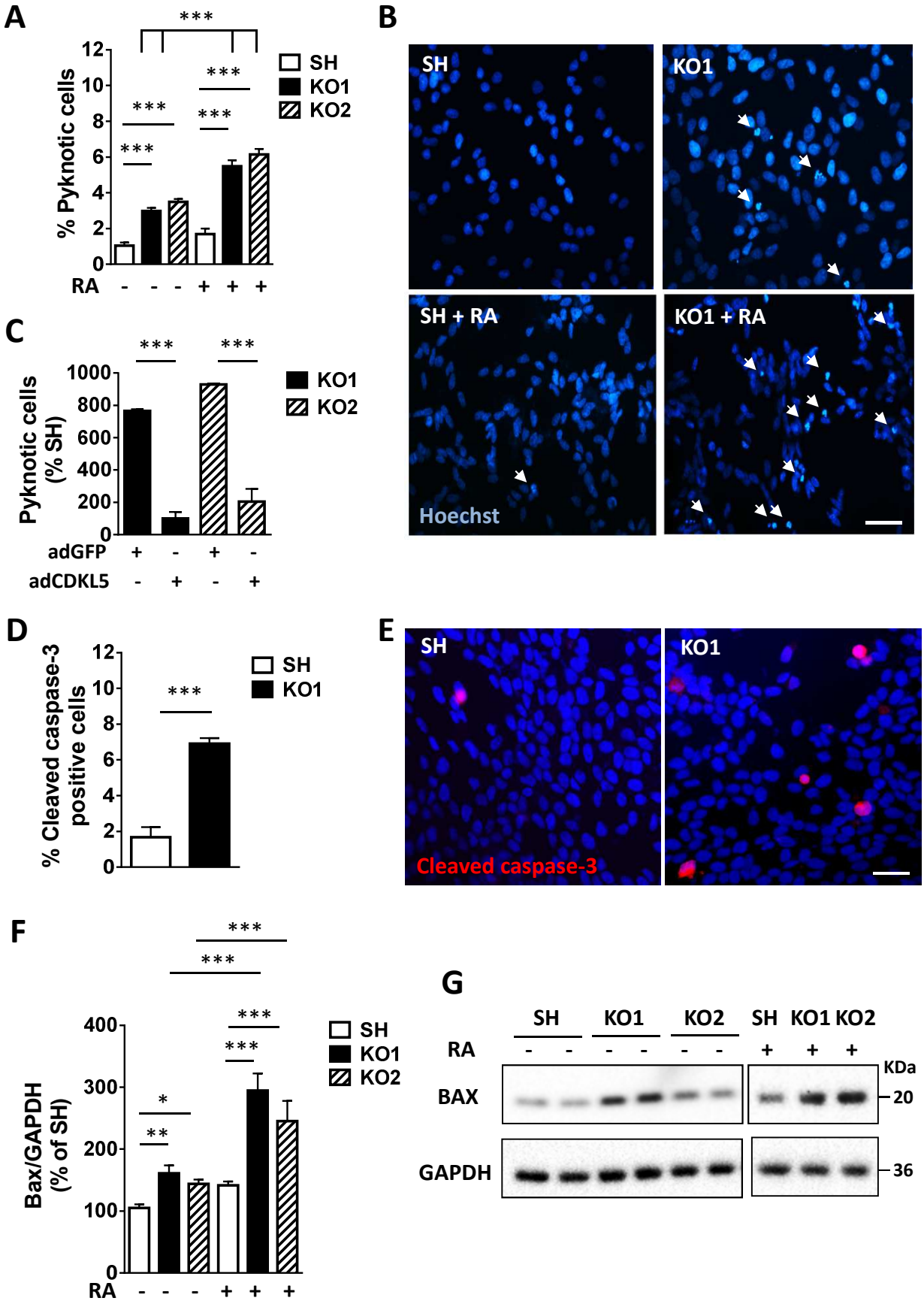
A
% Pyknotic cells
SH
KO1
KO2
RA
B
SH
KO1
SH + RA
KO1 + RA
Hoechst
C
Pyknotic cells (% SH)
KO1
KO2
adGFP
adCDKL5
D
% Cleaved caspase-3 positive cells
SH
KO1
E
SH
KO1
Cleaved caspase-3
F
Bax/GAPDH (% of SH)
SH
KO1
KO2
RA
G
SH
KO1
KO2
SH
KO1
KO2
RA
BAX
GAPDH
KDa
20
36

Figure 4

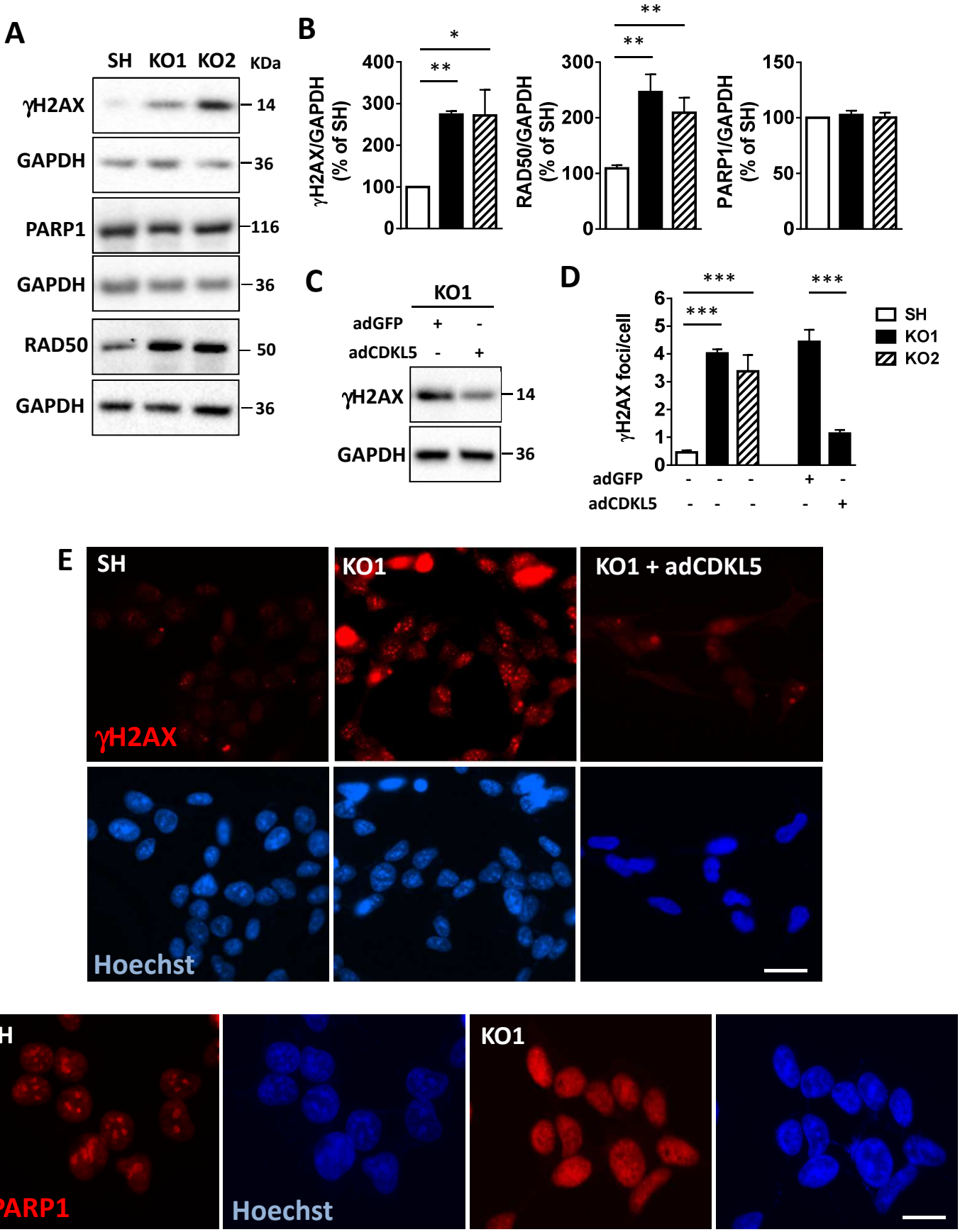
A
SH
KO1
KO2
KDa
γH2AX
14
GAPDH
36
PARP1
116
GAPDH
36
RAD50
50
GAPDH
36
B
γH2AX/GAPDH (% of SH)
RAD50/GAPDH (% of SH)
PARP1/GAPDH (% of SH)
C
KO1
adGFP
adCDKL5
γH2AX
14
GAPDH
36
D
γH2AX foci/cell
SH
KO1
KO2
adGFP
adCDKL5
E
SH
KO1
KO1 + adCDKL5
γH2AX
Hoechst
F
SH
KO1
PARP1
Hoechst

Figure 5

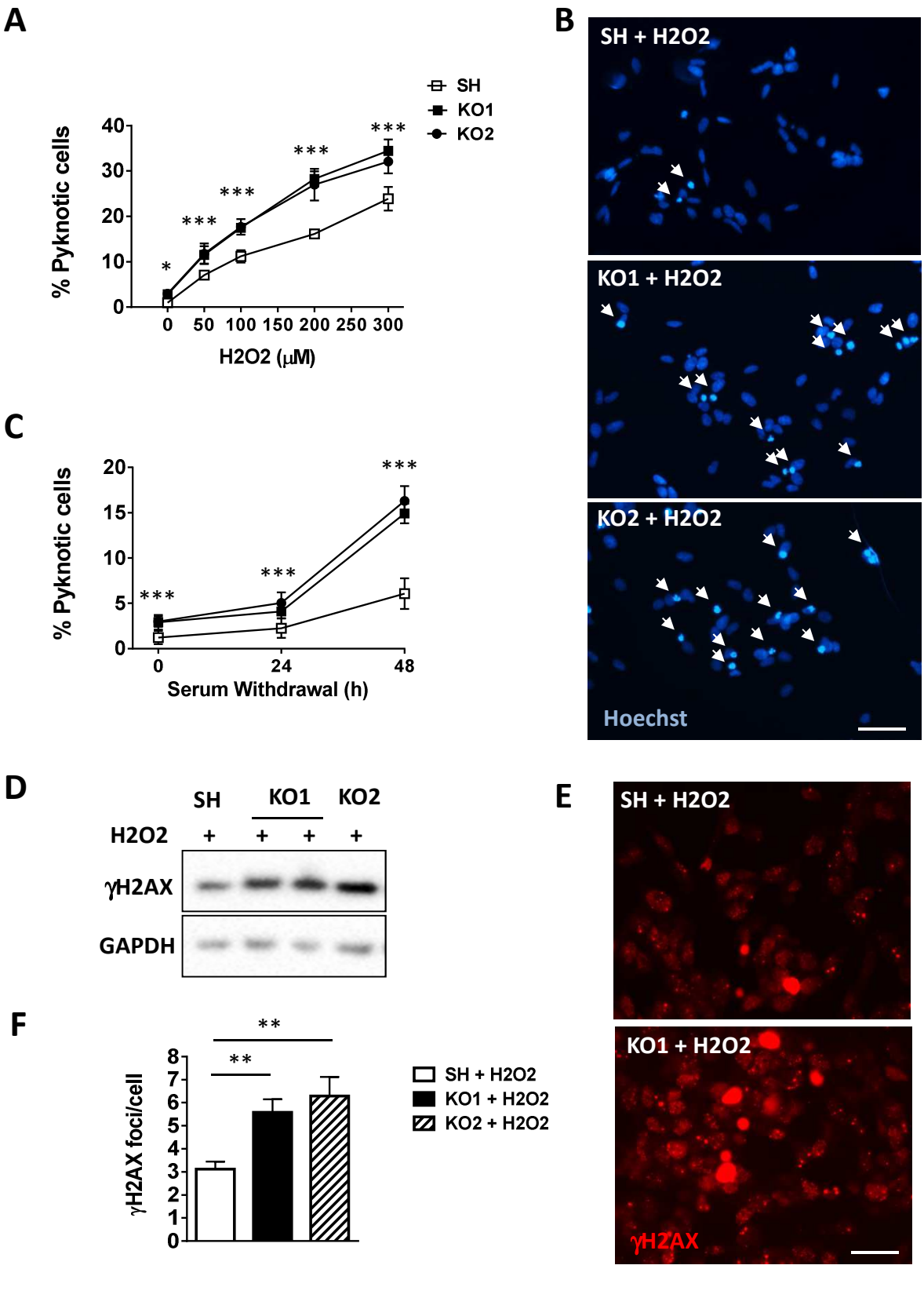
A
SH
KO1
KO2
% Pyknotic cells
H2O2 (μM)
B
SH + H2O2
KO1 + H2O2
KO2 + H2O2
Hoechst
C
% Pyknotic cells
Serum Withdrawal (h)
D
SH
KO1
KO2
H2O2
γH2AX
GAPDH
E
SH + H2O2
KO1 + H2O2
γH2AX
F
γH2AX foci/cell
SH + H2O2
KO1 + H2O2
KO2 + H2O2

Figure 6

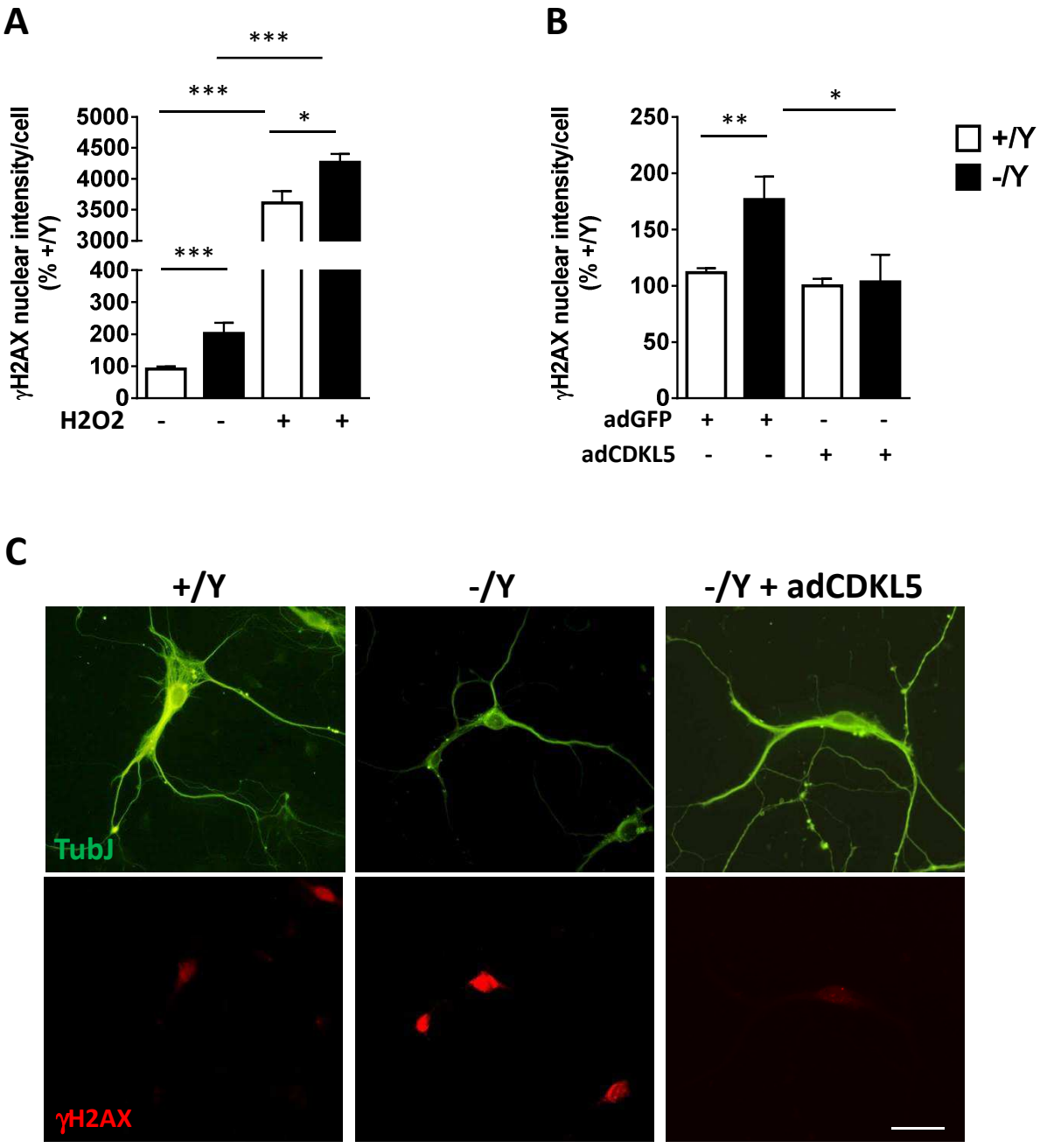
A
***
***
*
***
γH2AX nuclear intensity/cell (% +/Y)
5000
4500
4000
3500
3000
400
300
200
100
0
H2O2 - - + +
B
**
*
250
200
150
100
50
0
adGFP + + - -
adCDKL5 - - + +
+/Y
-/Y
C
+/Y
-/Y
-/Y + adCDKL5
TubJ
γH2AX

Figure 7

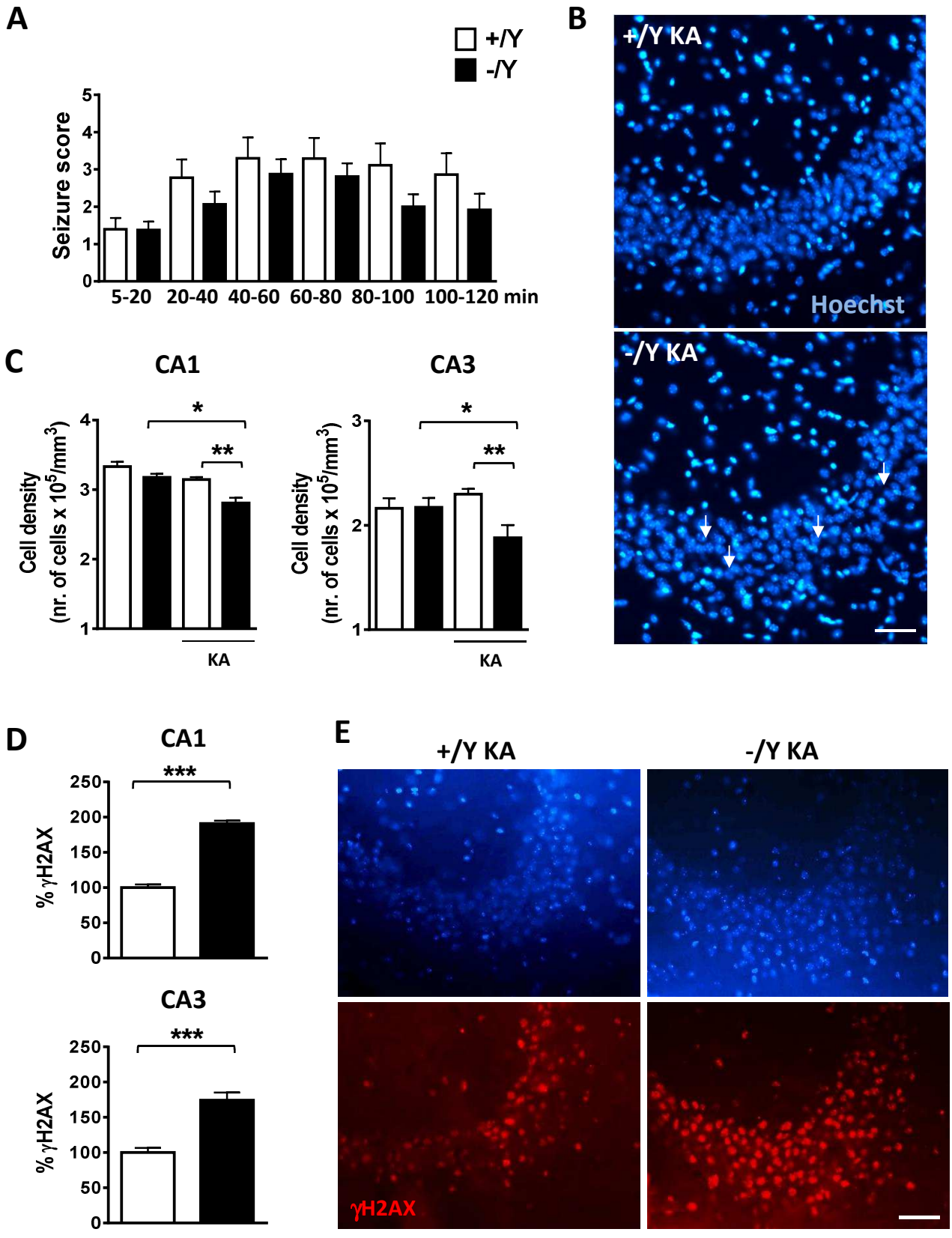
A
+/Y
-/Y
Seizure score
5-20
20-40
40-60
60-80
80-100
100-120 min
B
+/Y KA
Hoechst
-/Y KA
C
CA1
CA3
Cell density
(nr. of cells x 10^5/mm^3)
*
**
KA
D
CA1
CA3
***
% γH2AX
E
+/Y KA
-/Y KA
γH2AX

Figure 8

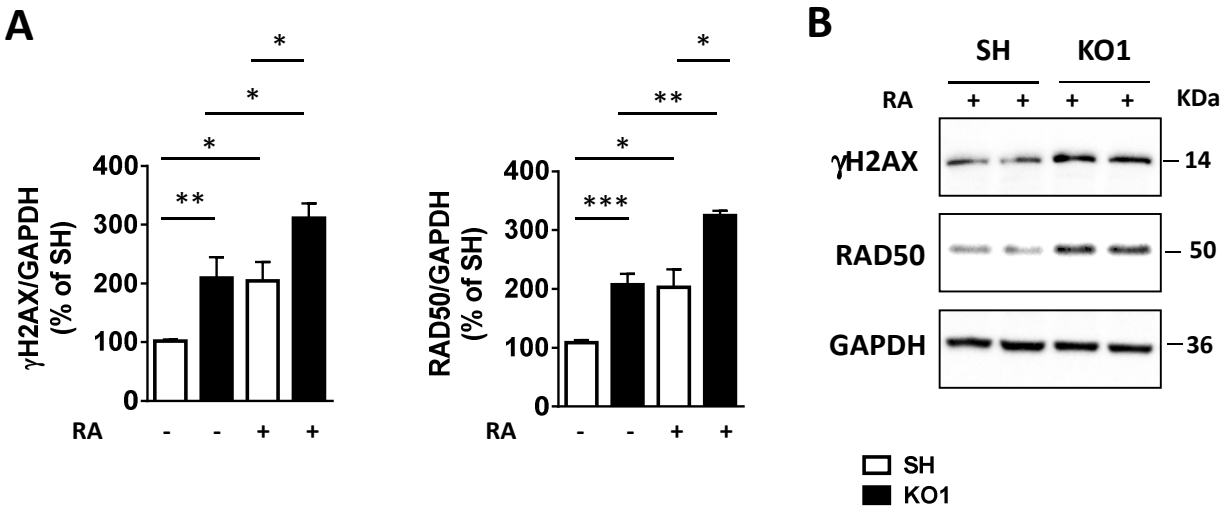

Supplementary Figure 1.

A: Western blot analysis of gH2AX and RAD50 levels normalized to GAPDH levels in protein extracts from undifferentiated (SH and KO1) and RA-differentiated (SH + RA and KO1 + RA) cells. **B:** Examples of immunoblots of samples as in A.